Nuclear Physics and Engineering (2018) 1(2):1–5

Nuclear Physics and Engineering

An International Peer-Reviewed Journal (http://npe.kntu.ac.ir)

Investigation the effect of anode's insert material on spatial distribution of X-ray source in plasma focus device

Seyed Milad Miremad, Babak Shirani Bidabadi*

Department of Nuclear Engineering, Faculty of Advanced Science & Technologies, University of Isfahan, Isfahan, Iran
*Corresponding author: b.shirani@ast.ui.ac.ir

HIGHLIGHTS

- X-ray emitting zone changes with gas pressure and anode's insert metal.
- Spatial distribution of X-rays from anode's surface depends on the characteristics of the electron beam.
- Spatial distribution of X-rays from the plasma above the anode depends on properties of the working gas.
- Size and intensity of X-ray source increases with atomic number of the insert materials.

ABSTRACT

In this paper, the effect of anode's insert material on spatial distribution of X-ray emission zone of plasma focus device was studied. Anode's insert materials were fabricated out of aluminum, zinc, tin, tungsten and lead. For each insert material at the constant operating voltage of 21 kV, the image of pinhole camera which monitors the surface and the top of anode was recorded at the various pressures of 0.3, 0.6, 0.9 and 1.2 mbar. The results indicated that the X-ray emission zone above the anode surface not only includes thermal radiation of plasma, but also depends on anode's insert materials. This zone could be due to the passage of high energy electrons from the vapor of anode's material above the anode's surface.

KEYWORDS

Plasma focus
Pulsed X-ray
Pinhole camera
Spatial distribution
Anode's insert

1 Introduction

A plasma focus (PF) device is able to produce a compressed dense and hot plasma at the end of the anode. The dynamics of the plasma focus operation can be physically described as follows: after the gas injection to the PF chamber at the appropriate pressure, a high voltage applies across the anode and the cathode and the gas breakdown occurs. At the end of breakdown phase, the two layers current sheath will be formed. The radial component of current density (J) and self-induced magnetic field in the azimuthal direction (B) (occurred Lorentz force (J×B)) cause the current sheath to accelerate axially in the axial phase. As the current sheath reaches the end of the electrodes, the radial compression phase starts. This phase can be divided into four phases which called radial inward shock, radial reflected shock, slow compression (quiescent) or pinch phase, and expanded column phase (Lee, 2014). After the slow compression phase, the radiations like neutron (if deuterium is used as the injected gas), ion particles, electron beam, and various electromagnetic radiations, from IR to X-ray, started and continued until the expanded column phase finished.

PF device has been found to be an intense source of pulsed X-ray. Because of very short X-ray pulses (∼100 ns) emitted from PF device, the measurement tools in this situation are limited. Intensity, energy spectrum, and the spatial distribution of X-rays emitted from PF can be controlled using various parameters such as type and pressure of injected gas, operating voltage and anode]s insert materials. The X-ray output from the plasma focus device can be used in many applications including X-ray imaging (Da Re et al., 2001; Moreno et al., 2001; Hussain et al., 2003a; Raspa et al., 2004; Pavez et al., 2014; Kanani et al., 2014), lithography (Kato et al., 1988; Kalaiselvi et al., 2014a,b), and medical applications (Tartari et al., 2004; Jain et al., 2016; Venere et al., 2001). In all of these applications, the spatial distribution of X-rays and their emission zone in PF device, and the effect of operation parameters as well are important.

Article history: Received 12 April 2018/ Revised manuscript received 2 May 2018/ Accepted 16 May 2018/ Available online 1 July 2018

The pinhole camera is an appropriate measurement tool for monitoring and studying the spatial distribution of PF pulsed X-rays. However, when the radiographic film is used as the detector in pinhole camera, the spatial distribution measurements are independent of time, but can be distinguished from time to time by using appropriate detectors of X-rays (Benedetti et al., 2016). Harris *et al.* (Harries et al., 1978) studied the location of soft and hard X-ray production in a plasma focus device and separated X-ray emissions considering two parameters of time and position. They reported that soft and hard X-rays are emitted from the plasma and from the tip of the central electrode, respectively. They also found that the plasma X-rays were emitted about 20 ns earlier than the tip of anode's X-rays (Harries et al., 1978). Owing to the fact that a large portion of the X-rays emitted from the plasma focus device are produced by the beam-target mechanism, the material of the anode's tip undoubtedly plays a decisive role in the emission of X-rays. Hussain *et al.* (Hussain et al., 2003b) studied the X-ray emission zone of a 1.8 kJ plasma focus device at the pressure of 0.5 mbar hydrogen gas by a pinhole camera. They placed the lead insert in the copper anode. In this circumstance, they separated the soft and hard X-ray areas by using the various filters on the pinhole camera's aperture, and recorded these areas on Fuji films. Moreover, Shafiq *et al.* (Shafiq et al., 2003) had investigated the characteristics of the X-ray emitted from the plasma focus device in different energy windows by inserting the discs of different metals in the tip of the anode. PIN-diodes with differential filters were used as a time-dependent detector and the pinhole camera was used for time-independent analysis. They showed that the X-ray emission is found predominantly as a result of electron beam activity on the anode tip.

In this research, attempts were made to study the effect of the material of anode's tip on X-ray zone. For this purpose, five metal inserts fabricated out of aluminum, zinc, tin, tungsten and lead were used. In constant capacitance charge voltage of 21 kV, one pinhole camera captured the X-ray emission zone at various pressures (0.3, 0.6, 0.9 and 1.2 mbar) of air injection gas for each of the inserts and further analyses were performed based on the images.

2 Laboratory layout

In this study, a 2.5 kJ Mather-type plasma focus device was employed. This device is supplied by an 11.4 μF capacitor with 21 kV charge voltage. The diameter and the effective length of central anode were 2.5 and 13 cm, respectively. Anode is made of copper that its tip was drilled about 1 cm in diameter and 2 cm in depth in a way that the insert materials could be embedded into this site. The insulator between the central electrode and six cathode rods is made of quartz. Five insert materials in a cylindrical form with a diameter of 1 cm were fabricated out of Al, Zn, Sn, W and Pb. These inserted materials were placed in the hole of the anode's tip such that their tips were at the same height of the anode's tip.

To record the image of pulsed X-ray spatial distribution emitted from the plasma focus device, one pinhole camera was used. Pinhole camera can offer an overview of the spatial position of X-ray emission zone, its approximate size, and a qualitative view of the radiation density of the X-ray source. The components of a prototype pinhole camera which has been used in this study are shown in Fig. 1.

Figure 1: The components of the pinhole camera which were used for studying the spatial distribution of X-ray emitted from plasma focus device.

Figure 2: Plasma focus device and assembled pinhole camera which installed on the wall of the chamber.

After assembling its components, the pinhole camera was installed on the wall of the chamber of PF devise, so that the anode surface and its top can be monitored as shown in Fig. 2.

The experiments were carried out using the 500 μm aperture and the magnification of cameras was adjusted to be unity. The images were recorded on Kodak E-speed

dental radiographic films. The darkness of the points on the film is proportional to the intensity and the energy of X-rays emitted from different parts of the X-ray emission zone. Because of different attenuation coefficients of filters for different energies, it should be noted that placing a filter between the aperture of pinhole camera and the radiographic film can complicate analysis of the X-rays spatial distribution. Accordingly, in this study no filter was used between the aperture and the radiographic film.

For the X-ray spatial distribution analysis, the recorded films were scanned at 1200 dpi resolution by a HP scanner. Then the images were analyzed by using the MATLAB image processing section. The analysis were carried out according to the average gray scale of the various parts of the images.

By placing different insert materials in the hole of the anode tip, the images of pinhole camera was recorded at four different pressures of injected air gas (0.3, 0.6, 0.9, and 1.2 mbar).

X-ray emitted from plasma focus device shows shot-to-shot variation, so integration of PF output over higher number of shots (in the same conditions) will be more predictable than the output of single shot.

Due to the high probability of saturation of the radiographic films in five shots, the optimum number of shots was chosen to be three for our experimental setup. In each experiment, the film was exposed to three consecutive successful shots in the same gas pressure, charge voltage, and anode insert. Each experiment repeated three times. The current derivative signal was measured using a Rogowski coil. The intensity of the pulse X-ray was measured using a scintillator detector (BC-400) placed 1.5 m in front of the Plexiglas window of PF chamber. The evidence to confirm the occurrence of a successful shot (pinch) is a sharp spike in the current derivative signal, as well as the observation of X-ray pulse by a scintillator detector.

3 Results and discussion

The results recorded by the pinhole camera for five different materials at four different pressures are shown in Fig. 3. X-ray emitted from the plasma focus device is mainly produced by two processes including thermal radiation of the plasma and radiation produced by the collision of high-energy electron beams with the anode surface. Two X-ray emission regions are therefore considered: One on the anode surface (similar to a line in Fig. 3), and the other above the anode surface (similar to a cloudy cone shape in Fig. 3). The hot and dense plasma produced in the PF device is the source of X-rays. Three types of electron transition including bound-bound, free-bound and free-free emit X-ray from the plasma. These radiations are called plasma thermal radiation. In addition, in a plasma with a strong magnetic field, such as that used to form a pinch plasma, there would be another type of emission called cyclotron radiation. The radiation caused by the collision of the accelerated electron beam in the electric field which was created in the pinch region with the anode surface, contains both discrete and continuous components. Characteristic X-rays and Bremsstrahlung radiations are discrete and continuous components of beam-target collisions, respectively.

At low pressure (0.3 mbar) of air injection gas, it has been observed that for anode's insert materials with low atomic number, such as aluminum (Z=13), zinc (Z=30) and tin (Z=50), X-ray emission zone is limited to the anode surface. X-ray emission from anode surface becomes thick at the pressure of 0.6 mbar. By further increase in pressure (0.9 mbar), the cloudy and cone shape of X-ray zone form above the surface of the anode, and this area becomes larger at a higher pressure (1.2 mbar). In the case of anode's insert materials with high atomic number such as tungsten (Z=74) and lead (Z=82), even at low pressures of working gas (0.3 mbar), the cloudy cone shape area above the anode surface is clearly observed. In these condition, the cloudy area is concentrated above the anode surface and its height is lessen by increasing the pressure.

The spatial distribution of X-rays emitted from the anode surface strongly depends on the intensity, the energy, and the dimensions of the electron beam. The intensity of the electron beam is proportional to the density of the electrons in the plasma. By considering constant current passing through the gas, increment of the gas pressure leads to increasing of swept mass of gas, and the density of the electrons as well. It is worthy to mention that in an optimal pressure which the plasma current reaches to the end of anode and the discharge current becomes maximum, the current passing through the plasma is maximum. The energy of the electron beam depends on the induction voltage in the plasma. This voltage itself depends on the variations of the inductance and the plasma current. The size of the electron beam depends on the pinch radius which relates to the magnetic pressure and the kinetic pressure in the column of the plasma.

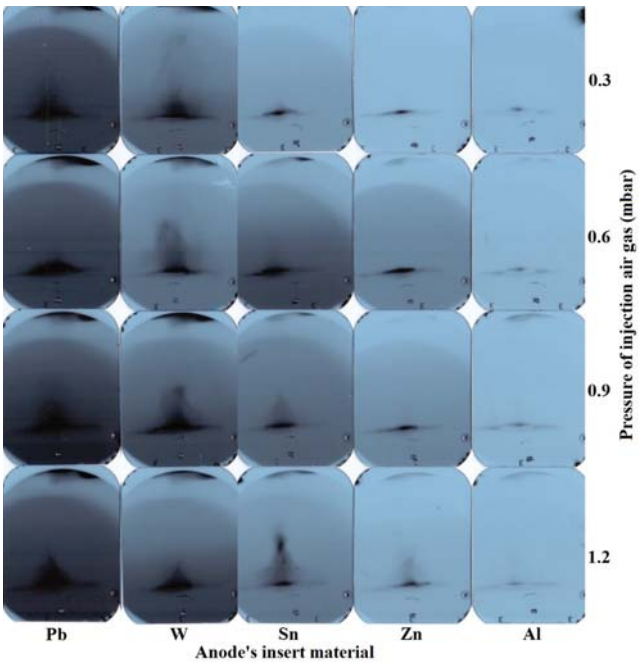

Figure 3: Digitized image of spatial distribution of X-ray emitted from plasma focus device with various anode's insert materials at different pressure of injection air gas.

Spatial distribution of X-rays emitted from the plasma above the surface of the anode depends on the properties of the plasma of injection gas, including the degree of ionization, plasma temperature, density of the electron and ion, and the radius and height of the pinch. The degree of ionization depends strongly on the type of gas. The smaller height and the radius of the pinch results in a denser plasma and a more darkening of the plasma region in the spatial distribution image.

According to the results obtained, it can be concluded that the X-rays emitted from the region above the surface of the anode are originated from the plasma of injected gas as well as the vapor of anode's material. In other words, at the same pressure of air gas, cone region above the surface of the anode is different for each anode's insert materials. It shows that the insert material affects the X-ray emission zone above the anode surface. The cloudy-cone region above the surface of the anode can be caused by production of metal vapor on the surface and the generation of X-rays due to the passage of electron beam through this vapor. Certainly, if the metal vapor can be produced in the device, the atomic density of zinc vapor or aluminum vapor should be far higher than that of tungsten which is a very rigid and hard metal with a high melting point.

The intensity of the Bremsstrahlung radiation directly relates to the atomic density of the target material. On the other hand, the intensity of the Bremsstrahlung radiation, and its average energy, increases by increasing the atomic number of the target material. The question is that which of the two mentioned factors (*i.e.* the vapor's atomic density and the atomic number) determines the intensity of X-ray source above the anode? The results of our experiments show that the intensity of X-ray source in the zone above the anode for tungsten, lead, and tin with high atomic numbers is significantly greater compared with two other metals. Therefore, the formation of metal vapor should also be happened even for tungsten with very high melting and boiling point. For a better understand of these observations, a perfect analysis of the mechanisms with governing the collision of the electron beam with the surface of metals should be considered. On the interaction between the high-energy electron beams of plasma focus with the surface of the anode's insert and conversion of the metal from solid to gas phase, three probable mechanisms can be considered: A) Transmission of energy by the electron beam to the metal's surface, elevation of the surface temperature, melting and then spreading out the melt by the physical strike of the electron beam, B) Elevation of the surface temperature and its sublimation, C) Physical evaporation by electronic sputtering.

Which of these mechanisms are predominant in the plasma focus device? The response of this question depends on the material, the energy of electrons, and the maximum thermal change of the surface of the anode. The boiling point of all of the studied anode's insert materials, even at the lowest operational pressure, is still greater than their general melting point, so that at the first, the surface of the metal melts definitely. Therefore, the mechanism B is ruled out. The melting of the metal's surface and collision of electron beam with the surface causes its dispersion and emission in the space above the anode and formation of a cloud of micro or nanoparticles in this zone. This mechanism is the most likely for lead and tin inserted anode with the lowest melting point.

Due to high melting point of tungsten, the damage of anode's surface after 18 shots was very trivial. However, the cloudy-cone shape region above the surface of the anode is bulky for tungsten. Therefore, the other probable mechanism, sputtering, should also be taken into consideration. The third mechanism is physical strike of high-energy electrons and dispersion of metal particles and formation of metal cloud above the anode for a short time. This mechanism does not cause a significant deformation of the metal surface. It can be shown that tungsten has a minimum sputtering threshold energy of 496 keV. This result gives the valuable information that a portion of the electrons produced in plasma focus device have energies more than 496 keV (Miremad and Bidabadi, 2018). The value of the sputtering threshold energy can therefore be an appropriate diagnostic tool for determining the upper range of the electron beam energy. Furthermore, the flux of these electrons is large enough so that tungsten vapor develops a powerful X-ray source in the zone above the anode.

It can be concluded that even if the three considered mechanisms are not dominant in generation of the anode vapor for a certain metal in comparison with others, the magnitude of its atomic number provides a more great effect on X-ray emitting from this gas vapor. This conclusion can be seen clearly in comparison of the X-ray emission zone of tungsten with aluminum or zinc. Considering aluminum as the insert metal with lowest atomic number, almost no X-ray emission zone was observed above the anode. X-ray emission from the anode surface was also very weak for aluminum.

4 Conclusion

Spatial distribution of X-rays emitted from plasma focus device develops from a linear zone on the anode tip (due to Bremsstrahlung radiation and characteristic X-ray from the anode surface) to a cloudy-cone shape above the anode. Changing in the pressure of injection gas and anode insert materials affect these regions. Significant differences were observed in the spatial distribution and intensity of the X-rays emitted from plasma focus device with different anode's insert materials. When the atomic number of the anode's insert material increases, the X-ray emission region extends from the radiation of the anode surface to the cloudy-cone shape above the surface of the anode, and the intensity of X-rays increases. Formation of a cloudy-cone shape above the anode can not be caused solely by the thermal radiation of the plasma, and relates to anode's insert material. It has been observed that at all pressures, the Bremsstrahlung radiation emitted from the anode surface and X-ray emitted from cone region above its surface increases by increasing the atomic number of anode's insert material. Also, given the gray scale of the images, it can be concluded that the dose recorded in the films was increased by increasing the atomic number.

References

Benedetti, L., Holder, J., Perkins, M., et al. (2016). Advances in X-ray framing cameras at the National Ignition Facility to improve quantitative precision in X-ray imaging. *Review of Scientific Instruments*, 87(2):023511.

Da Re, A., Mezzetti, F., Tartari, A., et al. (2001). Preliminary study on X-ray source from plasma focus device for fast radiography. *Nukleonika*, 46(suppl. 1):123–125.

Harries, W. L., Lee, J. H., and McFarland, D. R. (1978). Trajectories of high energy electrons in a plasma focus. *Plasma Physics*, 20(2):95.

Hussain, S., Ahmad, S., Khan, M., et al. (2003a). Plasma focus as a high intensity flash X-ray source for biological radiography. *Journal of Fusion Energy*, 22(3):195–200.

Hussain, S., Zakaullah, M., Ali, S., et al. (2003b). X-ray enhancement from a plasma focus by inserting lead at the anode tip. *Physics Letters A*, 319(1-2):181–187.

Jain, J., Moreno, J., Avaria, G., et al. (2016). Characterization of X-ray pulses from a hundred joules plasma focus to study its effects on cancer cells. In *Journal of Physics: Conference Series*, volume 720, page 012043. IOP Publishing.

Kalaiselvi, S., Tan, T., Talebitaher, A., et al. (2014a). Low-energy repetitive plasma focus based neon soft X-ray lithography source. In *Advances in X-Ray/EUV Optics and Components IX*, volume 9207, page 92070P. International Society for Optics and Photonics.

Kalaiselvi, S. M. P., Tan, T., Talebitaher, A., et al. (2014b). Optimization of neon soft X-ray emission from 200 j plasma focus device for application in soft X-ray lithography. In *International Journal of Modern Physics: Conference Series*, volume 32, page 1460323. World Scientific.

Kanani, A., Shirani, B., Jabbari, I., et al. (2014). Assessment of image quality in X-ray radiography imaging using a small plasma focus device. *Radiation Physics and Chemistry*, 101:59–65.

Kato, Y., Ochiai, I., Watanabe, Y., et al. (1988). Plasma focus X-ray source for lithography. *Journal of Vacuum Science & Technology B: Microelectronics Processing and Phenomena*, 6(1):195–198.

Lee, S. (2014). Plasma focus radiative model: Review of the lee model code. *Journal of Fusion Energy*, 33(4):319–335.

Miremad, S. M. and Bidabadi, B. S. (2018). Effect of inserted metal at anode tip on formation of pulsed X-ray emitting zone of plasma focus device. *Radiation Physics and Chemistry*, 145:58–63.

Moreno, C. H., Clausse, A., Martínez, J. F., et al. (2001). Ultrafast X-ray introspective imaging of metallic objects using a plasma focus. *Nukleonika*, 46.

Pavez, C., Zambra, M., Veloso, F., et al. (2014). Potentiality of a table top plasma focus as X-ray source: Radiographic applications. In *Journal of Physics: Conference Series*, volume 511, page 012028. IOP Publishing.

Raspa, V., Sigaut, L., Llovera, R., et al. (2004). Plasma focus as a powerful hard X-ray source for ultrafast imaging of moving metallic objects. *Brazilian Journal of Physics*, 34(4B):1696–1699.

Shafiq, M., Hussain, S., Waheed, A., et al. (2003). X-ray emission from a plasma focus with high-Z inserts at the anode tip. *Plasma Sources Science and Technology*, 12(2):199.

Tartari, A., Da Re, A., Mezzetti, F., et al. (2004). Feasibility of X-ray interstitial radiosurgery based on plasma focus device. *Nuclear Instruments and Methods in Physics Research Section B: Beam Interactions with Materials and Atoms*, 213:607–610.

Venere, M., Moreno, C. H., Clausse, A., et al. (2001). Tomographic system based on plasma focus X-rays. *Nukleonika*, 46.